

Decomposition of Surface EMG Signals

Carlo J. De Luca,^{1,3} Alexander Adam,¹ Robert Wotiz,² L. Donald Gilmore,¹ and S. Hamid Nawab^{2,3}

¹NeuroMuscular Research Center, ²Department of Electrical and Computer Engineering, and ³Department of Biomedical Engineering, Boston University, Boston, Massachusetts

Submitted 4 January 2006; accepted in final form 25 May 2006

De Luca, Carlo J., Alexander Adam, Robert Wotiz, L. Donald Gilmore, and S. Hamid Nawab. Decomposition of surface EMG signals. *J Neurophysiol* 96: 1646–1657, 2006; doi:10.1152/jn.00009.2006. This report describes an early version of a technique for decomposing surface electromyographic (sEMG) signals into the constituent motor unit (MU) action potential trains. A surface sensor array is used to collect four channels of differentially amplified EMG signals. The decomposition is achieved by a set of algorithms that uses a specially developed knowledge-based Artificial Intelligence framework. In the automatic mode the accuracy ranges from 75 to 91%. An Interactive Editor is used to increase the accuracy to >97% in signal epochs of about 30-s duration. The accuracy was verified by comparing the firings of action potentials from the EMG signals detected simultaneously by the surface sensor array and by a needle sensor. We have decomposed up to six MU action potential trains from the sEMG signal detected from the orbicularis oculi, platysma, and tibialis anterior muscles. However, the yield is generally low, with typically ≤ 5 MUs per contraction. Both the accuracy and the yield should increase as the algorithms are developed further. With this technique it is possible to investigate the behavior of MUs in muscles that are not easily studied by needle sensors. We found that the inverse relationship between the recruitment threshold and the firing rate previously reported for muscles innervated by spinal nerves is also present in the orbicularis oculi and the platysma, which are innervated by cranial nerves. However, these two muscles were found to have greater and more widespread values of firing rates than those of large limb muscles.

INTRODUCTION

The electromyographic (EMG) signal is composed of the action potentials from groups of muscle fibers organized into functional units called *motor units* (MUs). This signal can be detected with sensors placed on the surface of the skin or with needle or wire sensors introduced into the muscle tissue. When only two or three MUs in the vicinity of the sensors are active, it is usually possible to visually identify most of the individual MU action potentials because the incidence of superposition among the individual MU action potentials is relatively low. However, when the EMG signal contains the activity of four or more MUs the individual action potentials become, in large part, indistinguishable to the naked eye because the incidence of superposition among two or more MU action potentials becomes numerous and the shapes of the MU action potentials may approach in similarity.

In many cases it is desirable to study and/or use the information contained in the timing of the discharges of individual motor units, such as in investigations for furthering the understanding of how motor units are controlled by the CNS in

generating force or for assessing the degree of dysfunction in upper motoneuron diseases such as cerebral palsy, Parkinson's disease, amyotrophic lateral sclerosis (ALS), stroke, and other disorders. This may be achieved by "decomposing" the EMG signal. The concept is depicted in Fig. 1. A decomposed EMG signal provides all the information available in the EMG signal. The timing information provides a complete description of the interpulse interval, firing rate, and synchronization characteristics. The morphology of the shapes of the MU action potentials provides information concerning the anatomy and health of the muscle fibers.

From a practical perspective, it is desirable to obtain such information from the signal detected from a single sensor that is as unobtrusive as possible and that detects MU-rich EMG signals rather than a plurality of sensors that detect MU-poor EMG signals.

There have been numerous and varied approaches to extracting action potentials from neural and muscle activity over the past three decades. The mid-to-late 1960s produced a flurry of computer-based activity directed at identifying the individual action potentials and discharge times of neural activity by shape discrimination. Dominant among these pioneering attempts were the works of Gerstein and Clark (1964), Simon (1965), Keehn (1966), and Glaser and Marks (1966). Applications to separate the EMG signals did not appear until a full decade later (Andreassen 1983; De Figueiredo and Gerber 1983; De Luca and Forrest 1972; De Luca et al. 1982a,b; Guiheneuc et al. 1989; LeFever and De Luca 1978; Mambrito and De Luca 1984; McGill et al. 1985). This initial flurry was followed by sustained interest during the past two decades (Broman 1988; Christodoulou and Pattichis 1999; Fang et al., 1999; Hochstein et al. 2002; Iani et al. 1994; Jongen et al. 1996; Loudon et al. 1992; Nawab et al. 2004a,b; Stashuk and de Bruin 1988; Türker et al. 1989; Zennaro et al. 2001; among many others). To date all the above approaches and techniques that have been able to identify individual MU action potentials in the superimposed EMG signal and provide useful physiological information have used indwelling sensors to detect the signal. These types of sensors have obvious disadvantages arising from their invasive nature.

In this report we describe a successful attempt at accurately decomposing EMG signals detected from surface sensors.

BACKGROUND

For the past three decades we have been improving a technique that we have termed *Precision Decomposition I* (PD

Address for reprint requests and other correspondence: C. J. De Luca, NeuroMuscular Research Center, 19 Deerfield Street, Boston, MA 02215 (E-mail: cjd@bu.edu).

The costs of publication of this article were defrayed in part by the payment of page charges. The article must therefore be hereby marked "advertisement" in accordance with 18 U.S.C. Section 1734 solely to indicate this fact.

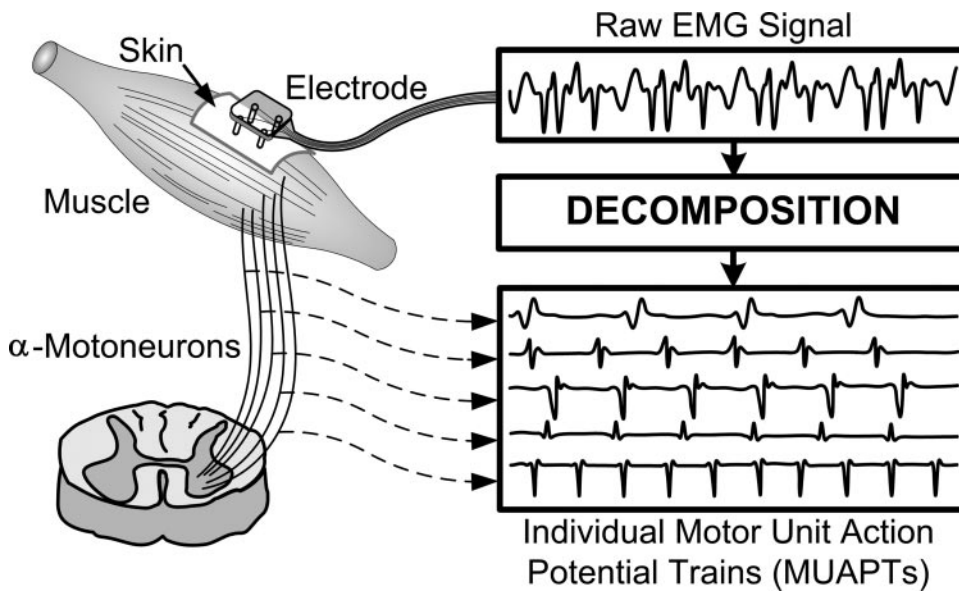


FIG. 1. Pictorial outline of the decomposition of the surface EMG signal into its constituent motor unit action potentials. (Adapted from De Luca et al. 1982a.)

I). The evolution of this technique, specifically designed to enable physiological experiments, has been described by LeFever and De Luca (1978), LeFever and De Luca (1982), Mambrito and De Luca (1984), Broman (1988), and De Luca and Adam (1999). The technique has been useful for decomposing indwelling EMG (iEMG) signals detected by needle sensors during isometric contractions and has been used in numerous physiological studies (see, e.g., Adam and De Luca 2003, 2005; Adam et al. 1998; De Luca et al. 1982a,b; Erim et al. 1999; Finsen et al. 2006; Kamen and De Luca 1989; Makasado et al. 1995; Masuda and De Luca 1991; Roark et al. 2002; Sogaard 1995; Westad and Westgaard 2005). Briefly, the technique consists of identifying action potentials in the iEMG signal and assigning them to specific motor units by classifying the shapes and amplitudes of the action potentials. The assignments of the action potentials are made on the basis of template matching and the probability of firing of the individual motor units being tracked. Slight modifications in the shape of the action potential can be tracked by adapting the templates to these modifications. Superpositions of action potentials are resolved. Artificial Intelligence techniques are used to accomplish all these tasks. These algorithms were able to decompose no more than eight MU action potential trains in the iEMG signal with an accuracy of 60 to 70% in an automatic mode, requiring 12-min processing time for 1-s acquisition time (De Luca et al. 1982a,b). The technique has provisions for using an Interactive Editor program to obtain decomposition accuracies of 100% in some records of EMG signals.

Throughout this communication, the decomposition accuracy for the *i*th decomposable motor unit train is defined as

$$A(i) = \frac{N_{FIR}(i) - N_{FN}(i) - N_{FP}(i)}{N_{FIR}(i)} \times 100\%$$

where $N_{FIR}(i)$ is the number of true firings of the MU and $N_{FN}(i)$ and $N_{FP}(i)$ are respectively the number of false negatives and the number of false positives produced by the decomposition algorithm for that MU. The term “true firings” refers to the firings that were obtained by an expert operator using the Interactive Editor on automatically decomposed data.

The overall decomposition accuracy for a signal with *N* decomposable MU trains is then obtained as

$$A = \frac{1}{N} \sum_{i=1}^N A(i)$$

The rationale behind this unweighted average is that the accurate decomposition of any MU train is of the same significance as that of any other MU train regardless of its duration, number of firings, and so forth.

Recently, we made significant improvements to the algorithms, rendering a considerably more powerful version that we have labeled *Precision Decomposition II* (PD II). The new algorithms are based on our own Artificial Intelligence knowledge-based approach specifically designed to manage signal-processing algorithms that perform two main categories of functions: 1) they identify differences in shapes and track changes in the shapes of the action potentials under a variety of conditions and 2) they resolve complex superpositions. The algorithms have been described in publications by Nawab and Lesser (1992), Winograd and Nawab (1995), Hochstein et al. (2002), and Nawab et al. (2004a,b). We succeeded in automatically decomposing iEMG signals from the quadrifilar needle sensor (De Luca et al. 1982a) and later with quadrifilar wire sensors (De Luca and Adam 1999) with typically 10 MU action potential trains with an accuracy of typically 85% with a processing time eightfold that of the acquisition time. In one extraordinary case we were able to decompose automatically an iEMG signal containing 14 MU action potential trains, of which the most significant eight could be detected with an accuracy of 98% (Nawab et al. 2004a).

The quadrifilar needle sensor has the advantage that it can be repositioned after an insertion or, if necessary, relocated, thereby increasing the probability of obtaining a quality signal that can be decomposed. The fine-wire version may be placed in deep muscles located under an overlying layer of muscle and it usually provides no discomfort once inserted; however, it has some disadvantages. Once inserted it cannot be precisely relocated within the muscle. One can pull the wire out fractions of a millimeter, although this procedure can be done only once

or twice and with little control over the precise placement of the sensor.

Both versions of sensors have inherent limitations:

- They must be inserted into the muscle. This requires a clinical preparation involving sterilization of the sensors and the environment where the insertion is to be made.
- They render difficult or, in some cases, preclude the investigation of MU firing properties in muscles located in sensitive and dangerous areas, such as the muscles of the lips, eyelids, tongue, and most facial muscles, as well as other regions.
- They carry the risk—albeit low—of infection and disease transmission.
- They cause minor damage to the muscle tissue from which they are detecting the signal, which in turn influences the shapes of the action potentials.
- They are not well tolerated by individuals who have needle aversion, such as children.
- Once these sensors are inserted, the subject must remain very steady. A minor movement of 0.1 mm may cause the shapes of the MU action potentials to change, thus precluding the continued identification of a specific unit and generally incapacitating the decomposition algorithms from identifying actions potentials in the remainder of the contraction.

Many of the disadvantages and limitations of indwelling sensors can be mitigated by developing technology that uses a sensor to detect the surface EMG (sEMG) signal and algorithms that can decompose the sEMG signal. Such an approach presents difficult challenges because the sEMG signal is more complex than that detected by the relatively more selective indwelling sensors.

The notion of decomposing the sEMG signal has been considered by many for two decades (e.g., Masuda et al. 1985) for the obvious reason that it can be used by nonclinical researchers interested in motor control. Kleine et al. (2000) were able to decompose up to five concurrently active MUs obtained in a multistep, highly user interactive template-matching procedure from surface EMG signals detected with a 128-channel sensor during a low-level (5%) maximal voluntary contraction (MVC). In the past two years, there has been increased interest in the problem of decomposing the sEMG signal. Östlund et al. (2004) and Holobar and Zazula (2004) investigated the problem with various signal-processing techniques, but the few results presented were restricted to contraction levels of $\leq 10\%$ MVC, included no direct measure of

accuracy, and assumed stationary MU action potential shapes and uncorrelated discharge behavior. Gazzoni et al. (2004) described a technique that automatically decomposes ≤ 10 simulated MU trains and detects, in select cases, two to three MU trains from real sEMG signals, but makes no attempt at decomposing superimposed action potentials. The PD I technique that we used two decades ago (LeFever and De Luca 1978) was similarly tested, with perfect results, on simulated EMG signals, but failed miserably when applied to real EMG signals. We argued the essential importance of testing decomposition techniques on real EMG signals in Mambrito and De Luca (1984). Most recently, Garcia et al. (2005) presented a semiautomatic decomposition algorithm to extract the average firing rates of one to two MUs from EMG signals detected with a surface electrode array. No accuracy measures for these results were given, but the authors provide a success rate of 19/26 complete firing trains for a set of synthetic EMG signals composed of ≤ 10 MU action potential trains.

In this report we describe a technology that is capable of decomposing several simultaneous MU action potential trains from real sEMG signals. Although it is in the early stages of development, we can demonstrate its efficacy. In some cases the present version of this new technology yields an accuracy similar to that obtained by our early algorithms of PD I using indwelling sensors. We refer to our new technique for the decomposition of sEMG signals as *Precision Decomposition III* (PD III). When fully developed, PD III should find applications in neurology, ergonomics, sports medicine, physical medicine, and space medicine.

METHODS

The surface sensor array

We chose a sensor design that was similar to that of the original needle sensor, but with larger dimensions. As shown in Fig. 2A, the sensor consists of four cylindrical probes (0.5 mm diameter) with blunted ends that protrude from the housing so that when pressed against the skin they make a surface indentation. The probes are placed at the corners of a 3.6×3.6 -mm square. The diameter of the probes was chosen to be as small as possible without piercing the skin when pressed forcefully. As in the intramuscular sensors mentioned above, each probe provides a detection surface. The leads are connected to the inputs of differential amplifiers. The four detection surfaces provide six differential combinations or channels. Signals from four of these channels are amplified and filtered with a bandwidth of 250 Hz to 2.0 kHz to remove any movement artifact at the low end of the spectrum and any excessively long tails of the action potentials. The signals are then stored. This arrangement is shown in Fig. 2B. We found that for the sEMG signals the use of four

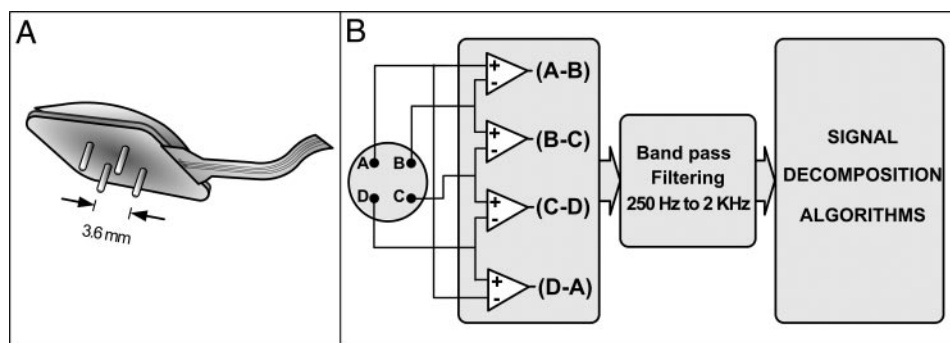


FIG. 2. A: surface electromyographic (sEMG) sensor array containing the 4 pins that detect the sEMG signals. B: differential combinations that produce 4 channels of sEMG signals. Detected signals from each channel are band-pass filtered before being decomposed by the algorithms.

differential channels improved the accuracy of the decomposition in PD III, whereas for iEMG signal decomposition in PD II, three differential channels were sufficient.

We arrived at the configuration and dimensions of the surface sensor array heuristically and are currently investigating other configurations. Ideally, the preferred array should maximize the difference in the detected shapes of the motor units while retaining physical dimensions that are sufficiently small so that it can be used on small muscles, such as those in the face, and is easy to manage when pressed against the skin.

Acquisition of sEMG signal

Three volunteers with no known neurological disorders participated in the tests. All subjects read and signed an informed consent form approved by the Institutional Review Board of Boston University. To detect the signal, the surface sensor array was pressed against the skin above the muscle of interest. No skin preparation or conductive gel was required. Sufficient pressure was applied to provide good electrical contact as evidenced by the best signal-to-noise ratio of the detected signals. (In our system, this is accomplished by viewing the detected signal on a computer screen in real time.) We detected signals from various muscles from the face, neck, and in limbs. Here we report on two muscles of the head and neck, the orbicularis oculi and the platysma, and on one limb muscle, the tibialis anterior. The head and neck muscles were chosen because they are not conveniently or comfortably assayed with a needle sensor and because their architecture differs from that of the more commonly studied limb muscles that have unified origins and insertions. The tibialis anterior was chosen as a typical representative of limb muscles. The sensor array was placed in the following locations. In the tibialis anterior, it was placed in the distal third (lengthwise) of the muscle; in the orbicularis oculi, it was placed on the lateral aspect of the superior eye lid; and in the platysma, it was placed on the lateral aspect of the neck, halfway between mandible and clavicle.

In the tibialis anterior, we recorded the torque output of the muscle and provided it as feedback to the subject so that a constant-force isometric contraction was generated during the detection of the sEMG signal to be decomposed. This was done by placing the limb in an apparatus that restrained the movement of the limb and was instrumented with a high-stiffness force gauge (model MB-250; Interface, Scottsdale, AZ). The torque output of the muscle generated during the contraction was expressed as a percentage of the maximal torque generated before the contraction. The subjects were asked to maintain a constant force at 20–50% MVC. In the muscles of the head and neck, where it was not possible to record the torque, the feedback to the subject was provided by the root-mean-squared (RMS) value of the EMG signal detected with a standard sEMG differential sensor (DE 2.1; Delsys, Boston, MA) placed adjacent to the array. This differential sensor consists of a parallel-bar configuration having detection surfaces that are 1 mm wide, 10 mm long, and spaced 10 mm apart. This sensor detects a global sEMG signal that is representative of the overall activity of the muscle being monitored. The global sEMG signal was detected with a bandwidth of 20–450 Hz and the RMS was calculated and smoothed using hardware circuitry. When processed in this fashion, the time-varying RMS value provides a reasonable analog to the force produced by the muscle (Basmajian and De Luca 1985; Lawrence and De Luca 1983). The time-varying value of the RMS of the global sEMG signal, or the estimated force, was expressed as a percentage of the value obtained during a maximal contraction. In the contraction of the orbicularis oculi, the subject was requested to squint with one eye and to attempt to maintain the global RMS constant. In the platysma, the subject was requested to tense the neck musculature and to maintain the global RMS constant.

Challenges of sEMG decomposition

Any approach for decomposing EMG signals must be able to deal with four major complexities that occur within the signal. These complexities are shown in Fig. 3: 1) *Superposition* of action potentials from different MUs, 2) *Large dynamic range* of the amplitudes among the action potentials of different MUs of interest, 3) *Shape changes* across the different action potentials of each MU (arising from slight movement between the sensor and muscle fibers and/or intracellular processes), and 4) *Similarity of shape* at various times among the action potentials of different MUs. These phenomena may also act in concert with each other to make the decomposition task all the more difficult.

These complexities are accentuated in the sEMG signal. Sample signals detected from the needle sensor and surface sensor array (shown in Fig. 2A) are presented in Fig. 4. The signals in this figure were obtained by inserting the needle sensor 1 cm beneath the surface sensor array, which was placed in the middle (lengthwise) of the tibialis anterior muscle. (Consequently, some of the action potentials in each signal belong to the same MUs.) It is visually apparent that the sEMG signal presents additional challenges for decomposition. First, there is the issue of *background clutter*. The greater detection volume of the array sensor leads to the sEMG signal containing action potential contributions from a larger number of MUs and those with smaller amplitudes will not be decomposable; they become part of the noise component of the signal. Second, there is the issue of *shape similarity*. The surface sensor array is located further away from the action potential sources and thus the shapes and amplitudes of the action potentials in the sEMG signal exhibit a smaller dynamic range; in other words, they appear to be more similar in shape and amplitude. Third, there is the augmented amount of *superposition* in the sEMG signal. The intervening inhomogeneous tissue between the skin and the action potential sources acts as a filter that, among other things, increases the time duration of the action potentials and therefore the amount of superposition.

Algorithms for decomposing sEMG signal

The PD III algorithms used to decompose the sEMG signal are modified versions of those previously developed by us for the PD II system (Hochstein et al., 2002; Nawab et al. 2002a,b, 2004a,b). The algorithms in both PD II and PD III are designed to address the difficulties inherent in trying to separate overlapping action potentials at various points in the EMG signal by using an Artificial Intelligence framework called *IPUS* (“Integrated Processing and Understanding of Signals”) Lesser et al. 1995; Nawab and Lesser 1992; Winograd and Nawab 1995). Although other signal-processing approaches have also been investigated for performing EMG decompositions, the IPUS approach has provided significantly more accurate results on intramuscular EMG data (Nawab et al. 2004a,b). The PD III system represents our initial attempt at incorporating the IPUS approach into the decomposition of surface EMG signals.

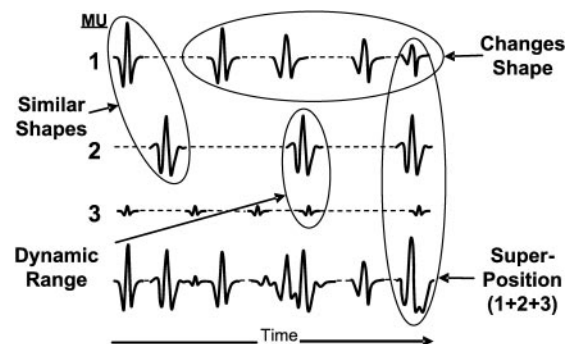


FIG. 3. Stylized examples of the various challenges presented by the realistic behavior of EMG signals detected with indwelling sensors with small detection volume and susceptible to movement.

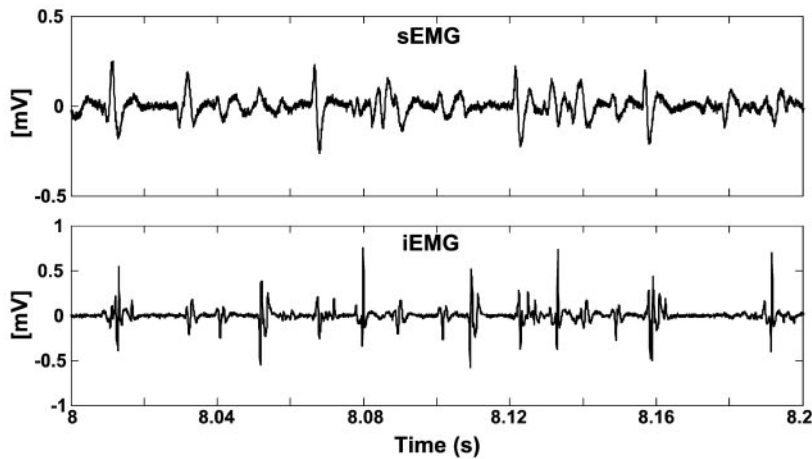


FIG. 4. *Top*: one channel of signal detected from the surface sensor array shown in Fig. 2A. *Bottom*: one channel of signal detected simultaneously from a needle quadrifilar sensor. Both signals were detected during constant 30% maximal voluntary contraction (MVC) isometric contractions from the tibialis anterior muscle.

As illustrated in Fig. 5, the PD III system consists of four processing stages. It takes as input a sEMG signal, $x(t)$, and produces as its final output a set $\{y^{(j)}(t) | j = 1, 2, \dots, N\}$ of N action potential trains. PD III first applies a digital IIR band-pass filter (see the APPENDIX for details) to the input EMG signal, $x(t)$, and passes the result, $x_B(t)$, through a maximum a posteriori probability (MAP) receiver (LeFever and De Luca 1982) designed to avoid false positives in the classification of action potential detections (see the APPENDIX for details). The MAP receiver may also be viewed as producing estimates $\{y_M^{(j)}(t) | j = 1, 2, \dots, N_M\}$ of N_M action potential trains. The corresponding decomposition error is evaluated as the square of the error signal, $e_M(t) = x_B(t) - \sum_{j=1}^{N_M} y_M^{(j)}(t)$. This error arises primarily because in trying to avoid false positives the MAP receiver 1) often splits off a motor unit train into two or more trains because of shape differences among various action potentials of the original train and 2) often fails to find a classification for signal data that is composed of complex superpositions of several different action potentials. Subsequent stages of processing are aimed at reducing these two types of decomposition error.

The third PD III stage shown in Fig. 5 is designed to avoid decomposition errors that arise because under certain conditions it is

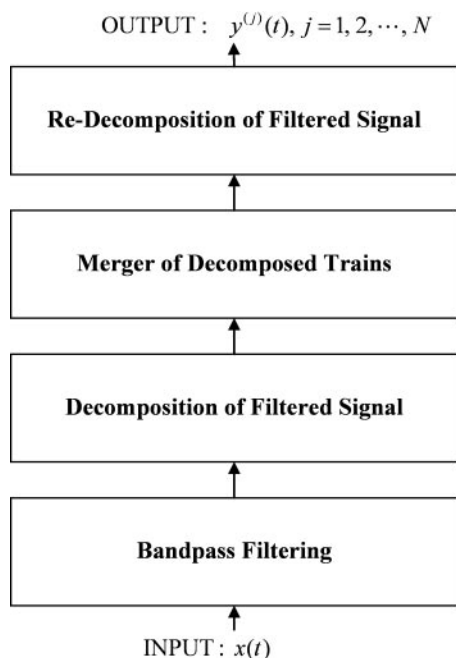


FIG. 5. Block diagram presenting the most important components of the Precision Decomposition III (PD III) algorithms.

possible for the MAP receiver to split the action potential train of a motor unit into two or more separate trains. This stage uses a “trellis traversal” search strategy (Castañón 1990) to identify trains that have a high probability of having been split off from other trains and merges them. The probability that a particular train may be “split off” from another train is estimated on the basis of the degree to which the template shapes of the two trains are correlated to each other and the degree to which they are uncorrelated to the template shapes of any other trains (see the APPENDIX for details).

The fourth PD III stage in Fig. 5 is designed to compensate for the ineffectiveness of the MAP receiver in signal regions involving complex superpositions. In such regions, significant interference between two or more action potentials makes the resultant data very different from any other data encountered in the input signal. In such cases, the MAP receiver declares the data as belonging to a new MU train but never finds a matching action potential later in the signal. Such “degenerate” trains are abandoned and their corresponding data are reanalyzed by PD III’s fourth stage. The reanalysis is aimed at identifying the nondegenerate trains from the MAP receiver that are consistent with the data in the superposition regions. This reanalysis begins with an iterative correlation strategy (see the APPENDIX for details) to assign probabilities of occurrence to each nondegenerate train in each superposition region. These iterative correlation results then undergo a utility maximization process (Von Neumann and Morgenstern 1944) to convert the probabilities of occurrence into decisions about which MU trains are actually consistent with the superposition data.

Interactive Editor

The results of the automatic decomposition could be improved by using the *Interactive Editor* to identify and correct wrongly assigned action potentials. Figure 6 shows an actual screen-shot of the pop-up window that appears in response to a click on a gap in the bar plot on the *top*, where each bar indicates a firing time of a motor unit. The pop-up window and its associated functions allow the user to compare the signal data in that gap with the various templates to determine whether there is sufficient evidence to indicate that the program made a mistake. In this particular instance, the operator judged that the signal data matched the visual characteristics of the motor unit with the gap in its bar plot. Consequently, the user was able to modify the decomposition results as indicated by the same MU’s bar plot at the *bottom* of Fig. 6. By using the interactive editor, it is possible to obtain decomposition accuracies that approach 100%.

RESULTS

Figure 7 shows a sample of the sEMG signal detected by the four channels of the sensor array along with the bar plots

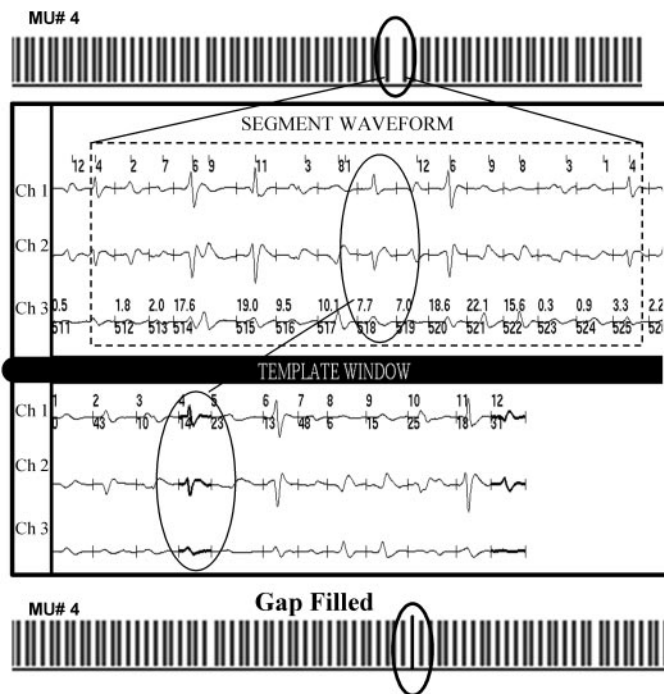


FIG. 6. Interactive Editor program. Motor unit (MU) train at the top contains an apparent error—the gap in the oval. By examining the underlying 3-channel EMG data it is possible to identify the unlabeled waveform as belonging to MU 4. Interactive Editor facilitates the decision-making process by providing local firing statistics for each motor unit, the ability to overlap a motor unit template with the signal waveform, and graphical representation of the residual signal energy after subtraction of the template.

identifying the location of the MU firings identified by the PD III algorithms. The signal was detected from the tibialis anterior muscle while the subject was performing an isometric contraction following a trapezoidal profile with a plateau of 50% MVC. The sEMG signal in each channel contains the action potentials emanating from the same source in the proximity of the detection surfaces, although the shapes will be different because of the location of each pair of detection surfaces with respect to the source. This difference in the action potential shapes is exploited by the decomposition algorithms to identify and classify the individual action potentials of a specific MU. This characteristic is useful for the PD III algorithms when action potentials superimpose and/or when the shapes change as a result of movement of the sensor with respect to the action potential source.

A dotted vertical line indicates the location of the identified action potential in the sEMG signal. Note that it is occasionally possible to visually identify individual action potentials, but for the most part visual identification is not possible because of superposition and considerable background noise. The sEMG signals contain more action potentials than those that are identified and tracked. The algorithms keep track of all the signals (above a selected threshold) to track the firings of the identified action potential trains. In this figure we show a short epoch of the firings of six MU action potential trains that were tracked continuously throughout the duration of the contraction. The PD III algorithms could sporadically identify the action potentials of other MUs throughout the contraction. The majority of the firings of the MUs with these sporadically identifiable firings could not be resolved by the Interactive

Editor and, consequently, they were abandoned because they provided little useful information. Figure 7 presents a segment of the contraction where the force is increasing and two MUs are recruited. The identification of new MUs is performed automatically. Also in the 0.5-s epoch presented, there are seven instances of superposition among the six concurrently active MUs. In one instance near the proximity of the 6.95-s mark, four MU action potentials superimposed and they were correctly identified.

The remainder of the decomposition of the trapezoid contraction is presented in Fig. 8. This is the result of the edited version, which required 12 h of expert user interaction. The automatic decomposition was obtained in 8 min with an accuracy of 90.4%. Figure 8A presents all the firings of six MUs throughout the complete duration of the 25-s-long contraction. (We refer to this as the *Bar Plot*.) The dark line represents the force produced by the subject. The arrows on the force axis indicate the recruitment threshold of the MUs. Figure 8B presents the interpulse interval, plotted vertically for each firing of all the MUs. (We refer to this as the *Dot Plot*.) This presentation is useful for visually identifying the errors in the decomposition, which are seen as dots that fall either noticeably below or above the average firing interval. Figure 8C presents the time-varying mean firing rates of each MU. The time-varying mean firing rates are obtained by passing the impulse trains corresponding to the firing trains of the *top plot* through a unit-area Hanning filter of 1.0-s duration. The decreasing firing rate value as a function of time during the constant force contraction is consistent with similar previous observations by De Luca et al. (1996). The shapes of the action potentials of the MUs for all four channels are presented in Fig. 8D. The shapes fluctuated throughout the contraction. The thick line represents the mean value of the amplitude of the action potentials and the thin, dashed lines above and below represent the SD.

Several contractions from the platysma and the orbicularis oculi were decomposed. In one case, we obtained an accuracy of 91.3% from the automatic decomposition. Examples of these decomposition results are shown in Fig. 9. In this figure we present the edited firing times and time-varying mean firing rates of the decomposed action potentials for identified MUs from the orbicularis oculi and the platysma, along with the estimated force by the RMS value of the global EMG signal. These examples are typical of the current capability of rudimentary PD III.

Note that the contraction of the tibialis anterior (Fig. 8) was relatively constant, whereas the contractions of the other two muscles were more erratic (Fig. 9). The study participants could not perform smooth sustained contractions with their facial and neck muscles, such that the RMS of the EMG signal fluctuated substantially. The fact that the signals could be decomposed under this condition is a testament to the ability of PD III.

Proof of accuracy and consistency

When one proposes to decompose a signal whose composition is not known a priori, it is incumbent on the proponent to prove that the decomposition is performed accurately. In our case it is also necessary to provide evidence that the rudimentary PD III decomposition technique provides information

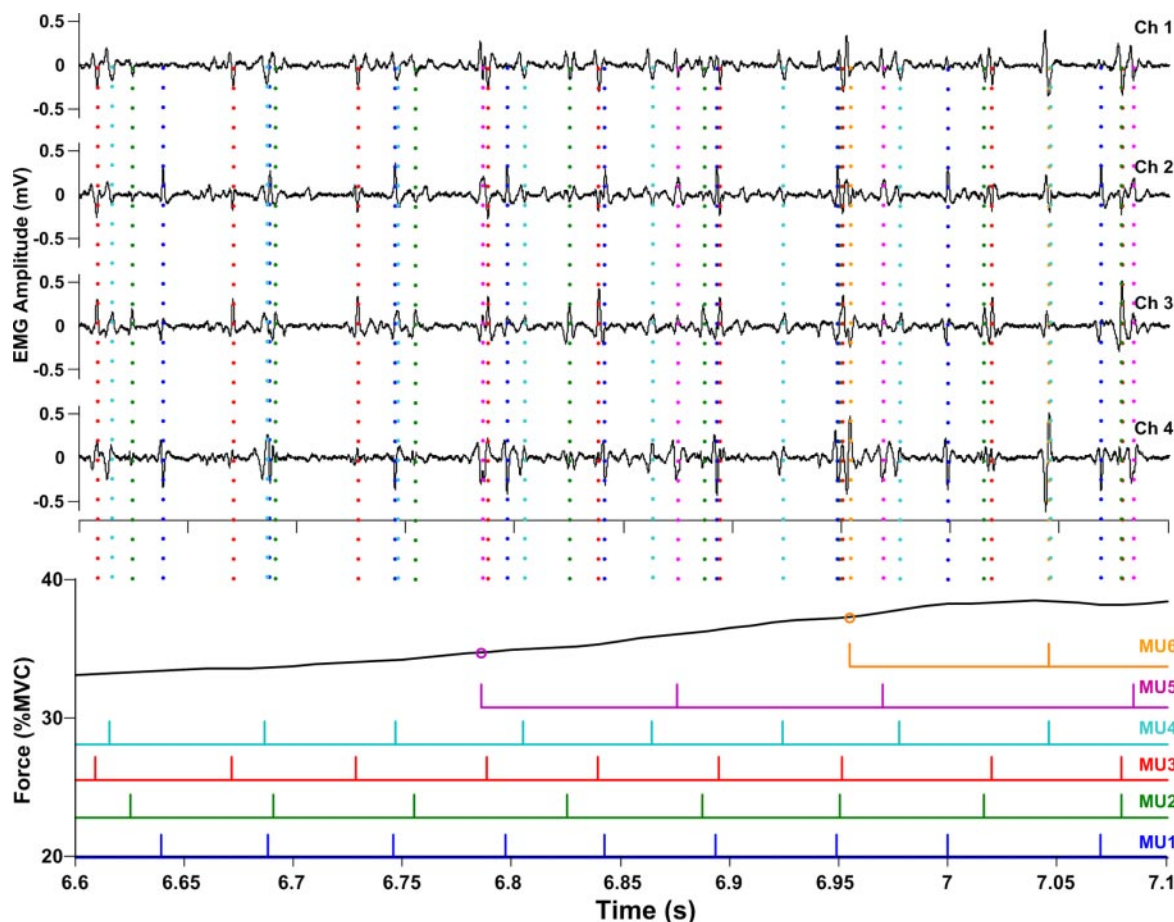


FIG. 7. *Top*: examples of the 4 channels of the sEMG signals detected by the surface array sensor from the tibialis anterior muscle during a 50% MVC contraction. Dotted vertical lines indicate the location of identified motor unit action potentials. *Bottom*: firing times of 6 motor units extracted from the decomposed sEMG signals above. Note that the location of the action potentials indicated by the bars corresponds to the identifiable pulses in each channel of the sEMG signals. Algorithms were able to identify the recruitment of MU 5 and MU 6, events that are not visually recognizable in the sEMG signals. Also, the algorithms resolved 7 cases of superpositions that are not obvious from the appearance of the sEMG signals.

similar to that of the more established PD II technique, which decomposes the iEMG signal detected with indwelling sensors. One obvious approach for proving accuracy would be to construct mathematically a signal of known components (MU action potential trains) and then proceed to decompose the synthesized signal into the constituent action potentials and check the veracity of the outcome. Over two decades ago Mambrito and De Luca (1984) showed that if the shapes of the action potentials remain invariant throughout the contraction, this approach is not sufficiently challenging, even when white noise having an amplitude 20% of the average amplitude of the action potentials was added to the signal. The challenges presented by real signals and identified in the preceding section represent important complexities that must be dealt with. Additionally, the algorithms must be able to cope with other unforeseen signal components that are occasionally presented by real data as a result of abrupt displacements of the sensor with respect to the source of the action potentials. Consequently, we used the “two-source” technique that we first introduced in 1984.

We placed a surface sensor array (Fig. 2A) on the skin above the tibialis anterior muscle and a quadrifilar needle sensor was inserted directly beneath the array sensor, approximately 1 cm into the muscle. It was expected that some of the motor units

would contribute signals to both sensors and others to only one sensor, depending on the proximity of the muscle fibers to the separate sensors. The EMG signal from each sensor was automatically decomposed by the respective decomposition algorithm and then independently further processed with the assistance of the Interactive Editor. The firing times of the motor units from both sensors are shown in Fig. 10. Note that three of the five MUs decomposed from the iEMG signal were also found in the sEMG. The expanded time sequence in the middle indicates that the MUs are firing at precisely the same time. This was so for 97.6%, or 996 sEMG-detected out of 1,021 iEMG-detected firings of the three MU action potential trains. This proves that the rudimentary PD III can obtain the same information from the sEMG signal as the PDII obtains from the iEMG signal. The precise coincidence of all the action potentials in three trains extracted from the two signals also proves that both the PD II and the PD III decomposition algorithms are able to accurately decompose the signals because the probability that both algorithms make exactly the same errors in both signals is extremely small.

DISCUSSION

The first point is that it is possible to accurately decompose sEMG signals detected noninvasively by surface sensors, even

DECOMPOSITION OF SURFACE EMG SIGNALS

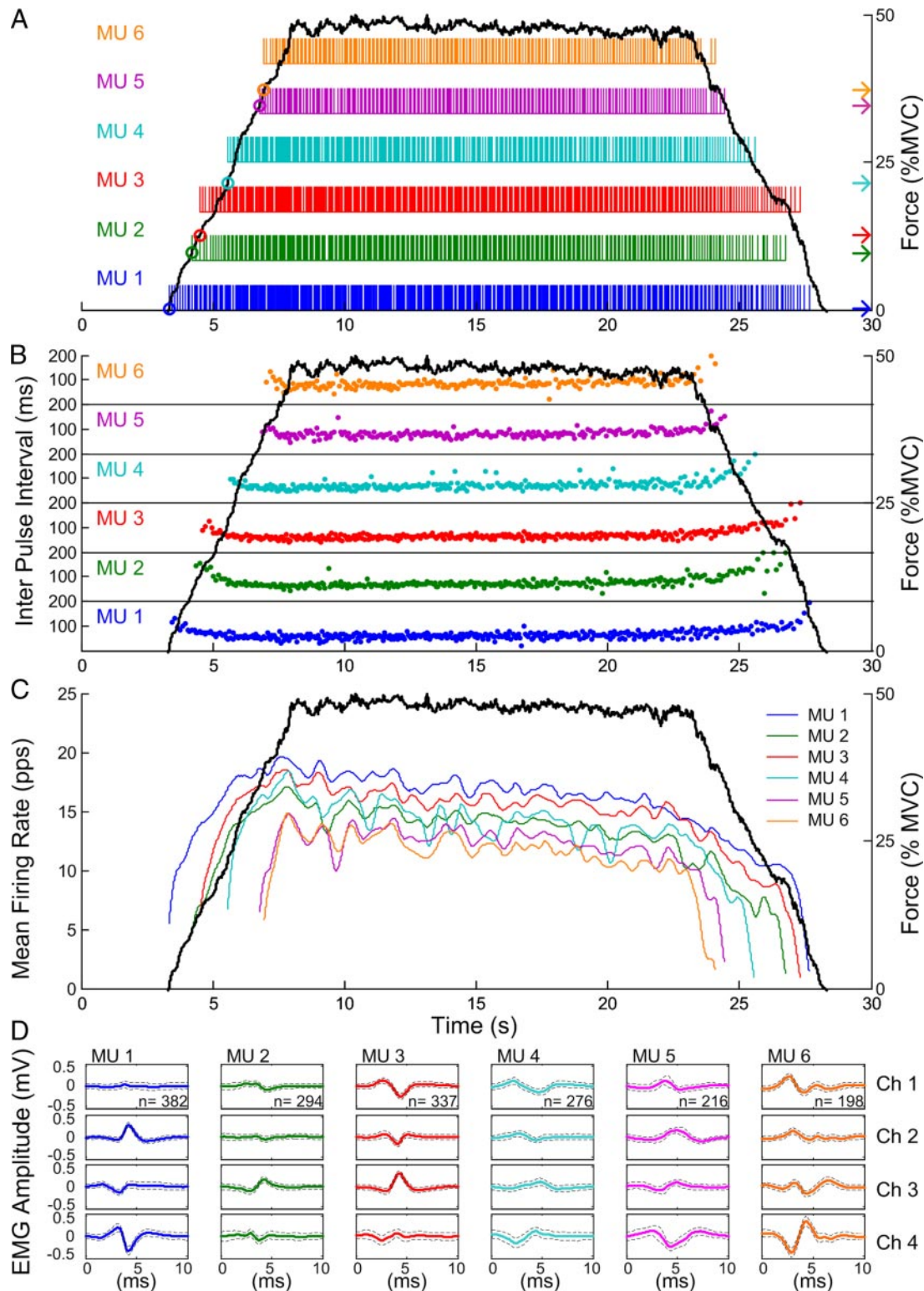


FIG. 8. Results of a decomposition of the sEMG signal detected from the tibialis anterior muscle during a 50% MVC contraction. This automatic decomposition yielded an accuracy of 90.4% of the presented data, which was edited with Interactive Editor. *A*: bar plot of the individual firings of 6 concurrently active motor units. *Continuous trace* represents the isometric force generated by the subject. *B*: dot plot of the interpulse intervals of each motor unit. Vertical displacement indicates the time between adjacent firings. *C*: plot of the time-varying mean firing rates of each motor unit. *D*: shapes of the action potentials of 6 motor units as recovered from the raw sEMG signal through spike-triggered averaging. Mean (solid line) \pm SD (dashed line) are plotted for each action potential.

for unstable contractions $\leq 50\%$ MVC. The algorithms were able to automatically identify the recruitment and the derecruitment of MUs. This is an important feature of our system that

is particularly relevant for physiological studies where the presence of new MUs imparts physiological meaning. No other reported attempt at decomposing the sEMG signal has made

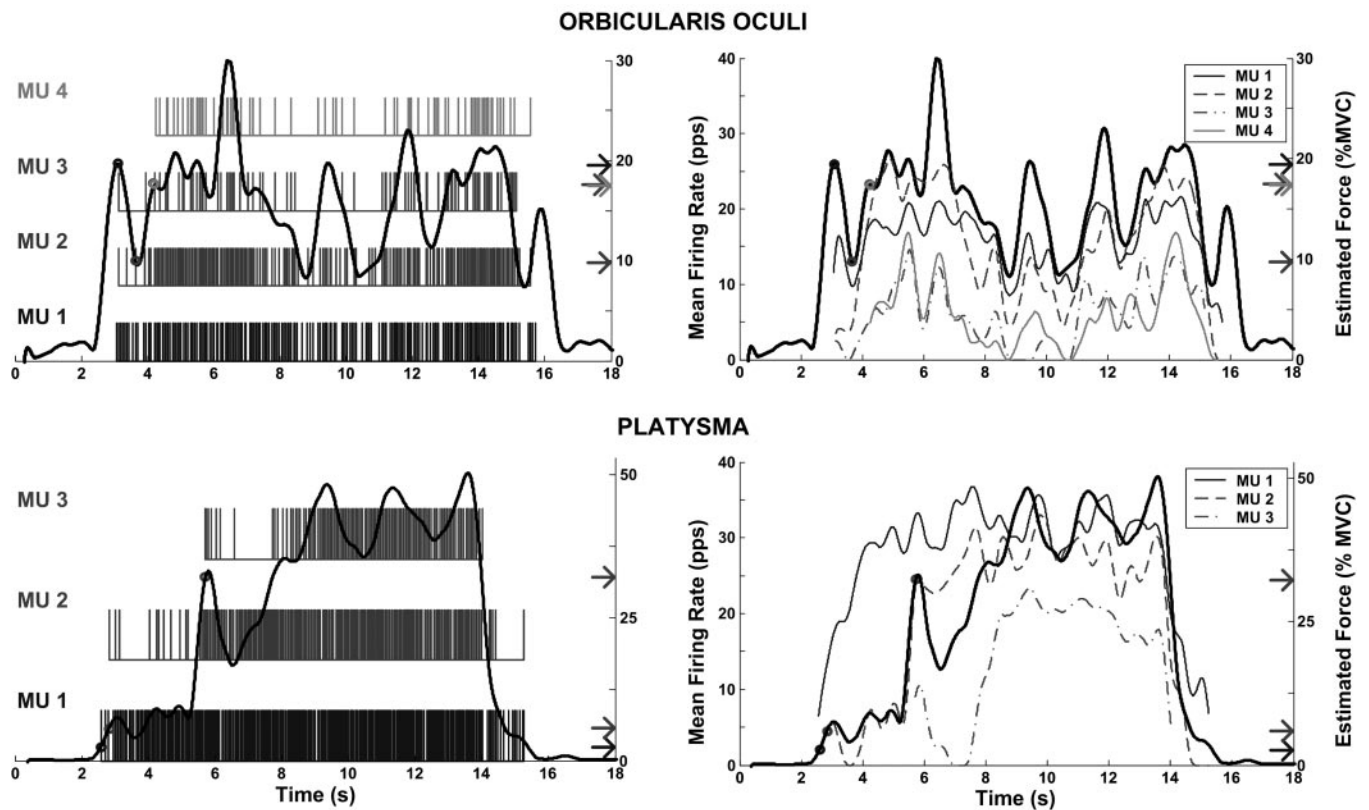


FIG. 9. Results of sEMG decomposition from the orbicularis oculi and platysma. Data are examples of motor unit firing patterns during a 30 and a 50% MVC contraction from one subject. Plots on the *left* present the firing times of motor units; plots on the *right* represent the time-varying mean firing rates of the motor units. Solid black lines represent the root-mean-squared value of the EMG signal detected with standard surface sensors, which provides an indication of the force exerted by the muscle (see text for details).

such claims. However, the MU yield in a contraction was low; it was typically less than five, compared with typically eight for iEMG signals, as previously reported in Nawab et al. (2004 a,b). Although the algorithms of the PD III are still rudimentary and the design of the sensor array was heuristic, we were able to extract at least three MU action potential trains from approximately one half of the sEMG signal records that were collected. We expect this yield to increase: 1) as the decomposition algorithms evolve to suit the specific characteristics of the challenges presented by the sEMG signal and 2) as the design of the sensor array evolves to provide channels that render signals with greater distinction in the shapes of the action potentials.

In addition to demonstrating a technical success, the decomposed data reveal two interesting physiological implications. The first concerns the behavior of the firing rates. It is noteworthy, that during a contraction the hierarchical organization of the firing rates of the orbicularis oculi and platysma, which are innervated by the VII cranial nerve, appears similar to that of the tibialis anterior, which is innervated by the L4, L5, and S1 spinal nerves. In particular, values of the mean firing rates of MUs are inversely proportional to their recruitment thresholds, such that earlier-recruited, low-threshold MUs maintain higher firing rates than later-recruited, higher-threshold units. (The occasional crossover between adjacent firing rates seen in Figs. 8 and 9 can be attributed to noise components in the

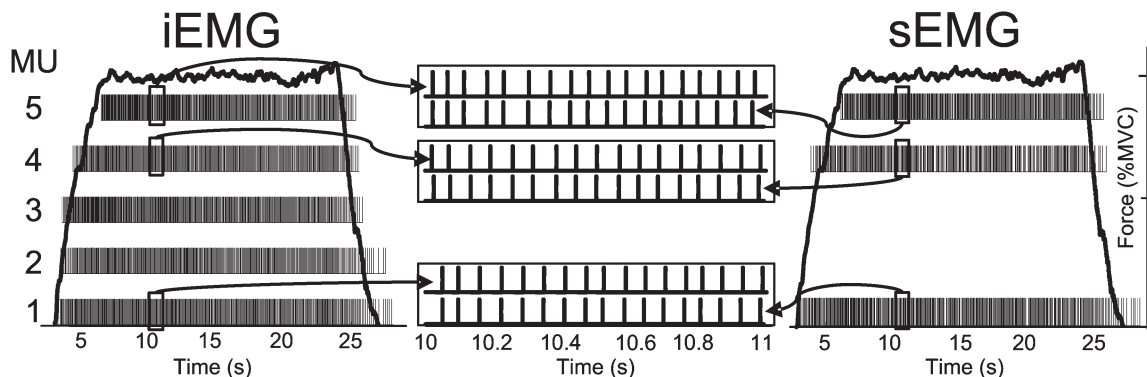


FIG. 10. Comparison of decomposition results of simultaneously recorded indwelling EMG (iEMG) and sEMG signals. Open spaces on the sEMG decomposition indicate some of the errors made by the algorithms. Note the perfect match for the motor unit firings in the expanded time interval.

common drive to the motoneuron pool.) The layered appearance of the plots of the firing rates versus force of successively recruited MUs led us to refer to this phenomenon as “onion skin” (De Luca and Erim 1994; De Luca et al. 1982a). This characteristic can be seen in data reported by other investigators who have signal processing knowledge (Freund et al. 1975; Hoffer et al. 1987; Masakado et al. 1995; McGill et al. 2005; Person and Kudina 1972; Rose and McGill 2001; Stashuk and De Bruin 1988). Some (Gydikov and Kosarov 1974; Moritz et al. 2005; Taylor and Enoka 2004) have argued against the hierarchical arrangement of the firing rates based on simulation studies or by combining the firing rate versus time curves of several subjects and/or contractions and emphasizing the lack of the hierarchical arrangement. Clearly the latter approach introduces intrasubject variations and cannot be used to describe the relative behavior of firing rates present within a contraction.

The second implication is that the dynamic range of the firing rate of MUs innervated from the cranial nerves (i.e., the orbicularis oculi and the platysma) is similar to that of the small muscles of the hand, which are innervated by the cervical nerves. De Luca et al. (1982a) reported that the firing rates of the first dorsal interosseous reached values of 41 pps; Kukulka and Clamann (1981) and Bigland-Ritchie et al. (1983) reported those of the adductor pollicis to reach 32 and 35 pps, respectively. These firing rate values are in contrast to those observed in large limb muscles, as exemplified by the tibialis anterior in this study and various other muscles in previously reported studies (Adam and De Luca 2005; De Luca and Erim 1994; De Luca et al. 1982a,b). In the two examples provided in Fig. 9, values of the firing rates of the orbicularis oculi and the platysma have a considerably greater spread among MUs of different recruitment threshold compared with the behavior of the MUs in the tibialis anterior (Fig. 8). Also the firing rates reach greater values in the orbicularis oculi and the platysma. For example, during the 50% MVC contractions, the firing rates of the platysma reach values of 35 pps, whereas those in the tibialis anterior reach about 17 pps. Although speculative, the higher dynamic range and absolute values of the firing rates of the orbicularis oculi and the platysma might be explained by a lack of recurrent inhibition by the Renshaw system. Its absence has been reported by Windhorst (1996) in the nearby oculomotor and masticatory muscles.

APPENDIX: SIGNAL PROCESSING DETAILS

Signal acquisition in PD III

- Number of signal channels: 4
- Sampling rate of input signal: 20,000 Hz
- Analog antialiasing filter: fourth-order Butterworth filter; 24 dB/octave slope; 9,500 Hz cutoff
- Analog high pass filter: second-order Butterworth filter; 12 dB/octave slope; 100 Hz cutoff

First stage of PD III

- Digital filter type: eighth-order Butterworth band-pass
- Digital filter's lower cutoff: 24 dB/octave <250 Hz
- Digital filter's upper cutoff: 24 dB/octave >2,000 Hz

Second stage of PD III

INPUT TO MAP RECEIVER. The input to the MAP receiver stage is a segmented version of $x_B(t)$, the filtered input signal. Each signal segment is established by virtue of its signal amplitudes being, on average, above a threshold that is determined adaptively by the decomposition system in accordance with a set of dynamic range criteria for the amplitudes of the decomposable MU trains. The segmented signal is then used to initiate and update action potential templates for each hypothesized MU. These templates are, in turn, used by the MAP receiver to help classify signal components that are detected by amplitude peaks in the segmented signal. The task of the MAP receiver is to associate a hypothesized MU with each detected signal component.

BASICS OF MAP RECEIVER. Denoting the i th MU by the symbol u_i , the MAP receiver assigns a particular MU, say, u_k , to the signal component such that

$$P(u_k|\rho) > P(u_i|\rho) \quad 1 \leq i \leq M, i \neq k$$

where ρ is the data vector for the detected pulse. In the presence of white Gaussian noise with variance σ^2 , the MAP decision criterion may be stated as

$$|\rho - s_k|^2 - 2\sigma^2 \ln P(u_k) < |\rho - s_i|^2 - 2\sigma^2 \ln P(u_i) \quad 1 \leq i \leq M, i \neq k$$

where s_i is the data vector for the template of the i th MU, and $P(u_i)$ is the a priori probability that the detected pulse belongs to the pulse train u_i . This a priori probability is estimated by a hazard function calculation (LeFever and De Luca 1982), assuming that the first-order interpulse intervals have a Gaussian density for each MU.

TEMPLATE INITIATION. An EMG signal segment d is declared as an initiation of a new motor unit train if for each preexisting template s , the value α that minimizes $|d - \alpha s|^2$ is such that $|1 - \alpha| > 0.5$ or $|d - \alpha s|^2 / |s|^2 > 0.5$.

TEMPLATE UPDATE. When the MAP receiver determines a match between segment data d and a preexisting template s (old), the segment data are used to update the template in accordance with the recursive relation: s (new) = $\%s$ (old) + $\%d$. The initial template and all of its subsequent updates are saved for later use by the decomposition system.

Third stage of PD III

TEMPLATE SELECTION. When comparing two trains to determine whether they are both split off from a single train, the decomposition system selects the pair of templates (one from each train) that are closest in time to each other.

PROBABILITY ESTIMATION. In comparing template s_j with template s_k we estimate the probability that they are both from the same train as $P_{j,k} = \beta(s_j \cdot s_k) / (|s_j| |s_k|)$, where the \cdot symbol denotes the dot-product operation; $\beta = \alpha$ for $0 \leq \alpha \leq 1$, $\beta = 1/\alpha$ for $\alpha > 1$, $\beta = 0$ for $\alpha < 0$, and $\alpha = (s_j \cdot s_k) / (s_j \cdot s_j)$.

Fourth stage of PD III

The basic strategy is that a representative template for each MU train is correlated against the entire filtered signal. The representative template is selected as the one that was most recently updated. The goal is to determine locations where the “maximal amplitude” MU, i.e., the one whose representative template attains the greatest amplitude from among all the motor units, may be present. To achieve this goal, the receiver first determines the locations where the correlation function of the maximal MU has a local maximum that is greater than the correlation values at that point of all the other MUs. At each of the

determined locations, an estimate of the probability that the maximal MU's action potential actually occurred at the point is obtained as

$$\hat{P} = \beta(\sqrt{1 - |d - \alpha p|^2 / |d|^2})$$

where the template for the MU is represented by the vector p , the corresponding signal data are represented by the vector d , α is the scale factor that minimizes the value of $|d - \alpha p|^2$, and $\beta = \alpha$ if $0 \leq \alpha \leq 1$; $\beta = 1/\alpha$ if $\alpha > 1$; and $\beta = 0$ if $\alpha < 0$.

Conceptually, α represents the degree to which d and p are co-linear and $(d - \alpha p)$ represents the orthogonal component of the modeling error. A probability threshold is also established by the decomposition system as the largest probability value obtained by correlating the maximal-amplitude MU's template with the templates of the remaining MUs. At all the locations where the estimated probability is above the probability threshold, the template of the maximal MU (appropriately scaled) is subtracted from the sEMG signal to obtain the input signal for the next iteration. The next iteration is the same as the previous one except for the removal from consideration of the maximal MU of the previous iteration, thus leading to the declaration of another MU as the maximal MU for that iteration. Once all the iterations are complete, a utility maximization procedure is used for converting probabilities of occurrence into decisions about which MU may be actually responsible for which action potential contribution in the signal data.

ACKNOWLEDGMENTS

The authors thank A. Morgan and A. Trongnetrprunya for assistance in processing the data.

GRANTS

This work was supported by National Institutes of Health Bioengineering Research Partnership Grant 1R24HD-38585 from the National Center for Medical Rehabilitation Research of the National Institute of Child Health and Human Development, the National Aeronautics and Space Administration Grant NCC 9-127 and Delsys Inc.

REFERENCES

- Adam A and De Luca CJ. Recruitment order of motor units in human vastus lateralis muscle is maintained during fatiguing contractions. *J Neurophysiol* 90: 2919–2927, 2003.
- Adam A and De Luca CJ. Firing rates of motor units in human vastus lateralis muscle during fatiguing isometric contractions. *J Appl Physiol* 99: 268–280, 2005.
- Adam A, De Luca CJ, and Erim Z. Hand dominance and motor unit firing behavior. *J Neurophysiol* 80: 1373–1382, 1998.
- Andreasen S. Computerized analysis of motor unit firing. In: *Computer-Aided Electromyography*, edited by Desmedt JE. Basel: Karger, 1983, p. 150–163.
- Basmajian J and De Luca CJ. *Muscles Alive* (5th ed.). Baltimore, MD: Williams & Wilkins, 1985.
- Bigland-Ritchie B, Johansson R, Lippold O CJ, Smith S, and Woods JJ. Changes in motoneuron firing rates during sustained maximal voluntary contractions. *J Physiol* 340: 335–346, 1983.
- Broman H. Knowledge-based signal processing in the decomposition of myoelectric signals. *IEEE Trans Eng Med Biol* 7: 24–28, 1988.
- Castañón DA. Efficient algorithms for finding the K best paths through a trellis. *IEEE Trans Aerospace Electronic Syst* 26: 405–410, 1990.
- Christodoulou CI and Pattichis CS. Unsupervised pattern recognition for the classification of EMG signals. *IEEE Trans Biomed Eng* 46: 169–178, 1999.
- De Figueiredo RJP and Gerber A. Separation of superimposed signals by a cross-correlation method. *IEEE Trans Acoust Speech Signal Process* 31: 1084–1089, 1983.
- De Luca CJ and Adam A. Decomposition and analysis of intramuscular electromyographic signals. In: *Modern Techniques in Neuroscience Research*, edited by Windhorst U and Johansson H. Heidelberg, Germany: Springer-Verlag, 1999, p. 757–776.
- De Luca CJ and Erim Z. Common drive of motor units in regulation of muscle force. *Trends Neurosci* 17: 299–305, 1994.
- De Luca CJ, Foley PJ, and Erim Z. Motor unit control properties in constant-force isometric contractions. *J Neurophysiol* 76: 1503–1516, 1996.
- De Luca CJ and Forrest WJ. An electrode for recording single motor unit activity during strong muscle contractions. *IEEE Trans Biomed Eng* 19: 367–372, 1972.
- De Luca CJ, LeFever RS, McCue MP, and Xenakis AP. Behaviour of human motor units in different muscles during linearly varying contractions. *J Physiol* 329: 113–128, 1982a.
- De Luca CJ, LeFever RS, McCue MP, and Xenakis AP. Control scheme governing concurrently active human motor units during voluntary contractions. *J Physiol* 329: 129–142, 1982b.
- Erim Z, Beg MF, Burke D, and De Luca CJ. Effects of aging on motor-unit control properties. *J Neurophysiol* 82: 2081–2091, 1999.
- Fang J, Agarwal GC, and Shahani BT. Decomposition of multi-unit electromyographic signals. *IEEE Trans Biomed Eng* 46: 685–697, 1999.
- Finsen F, Sjøgaard K, Graven-Nielsen T, and Christensen H. Activity patterns of wrist extensor muscles during wrist extensions and deviations. *Muscle Nerve* 31: 242–251, 2005.
- Freund HJ, Budinggen HJ, and Dietz V. Activity of single motor units from human forearm muscles during voluntary isometric contractions. *J Neurophysiol* 38: 933–946, 1975.
- Garcia GA, Okuno R, and Akazawa K. Technological developments in Japan—a decomposition algorithm for surface electrode-array electromyogram: a noninvasive, three-step approach to analyze surface EMG signals. *Eng Med Biol Mag IEEE* 24: 63–72, 2005.
- Gazzoni M, Farina D, and Merletti R. A new method for the extraction and classification of single motor unit action potentials from surface EMG signals. *J Neurosci Methods* 136: 165–177, 2004.
- Gerstein GL and Clark WA. Simultaneous studies of firing patterns in several neurons. *Science* 143: 1325–1327, 1964.
- Glaser EM and Marks WB. The on-line separation of inter-leaved neuronal pulse sequences. *Rochester Conf. on Data Acquisition in Biology and Medicine*, 1966, p. 137–156.
- Guiheneuc P, Doncarli C, and Le Bastard M. Concomitant multitrain automatic analysis of motor unit potentials and macroEMG. In: *Computer-Aided Electromyography and Expert Systems*, edited by Desmedt JE. Amsterdam: Elsevier, 1989, p. 83–90.
- Gydkov A and Kosarov D. Some features of different motor units in human biceps brachii. *Pfluegers Arch* 347: 75–88, 1974.
- Hochstein L, Nawab SH, and Wotiz R. An AI-based software architecture for a biomedical application. *SCI-2002. Proc 6th World Multiconf Systemics Cybernetics, Informatics*, Orlando, FL, July 2002, vol. XI, p. 60–64.
- Hoffer JA, Sugano N, Loeb GE, Marks WB, O'Donovan MJ, and Pratt CA. Cat hindlimb motoneurons during locomotion. II. Normal activity patterns. *J Neurophysiol* 57: 530–553, 1987.
- Holobar A and Zazula D. Correlation-based decomposition of surface electromyograms at low contraction forces. *Med Biol Eng Comput* 42: 487–495, 2004.
- Iani C, Stalberg E, Falck B, and Bishoff C. New approaches to motor unit potential analysis. *Ital J Neurol Sci* 15: 447–459, 1994.
- Jongen PJH, Vingerhoets HM, Roelvelde K, and Stegeman DF. Automatic decomposition electromyography in idiopathic inflammatory myopathies. *J Neurol* 243: 79–85, 1996.
- Kamen G and De Luca CJ. Unusual motor unit firing behavior in older adults. *Brain Res* 482: 136–140, 1989.
- Keehn DG. An interactive spike separation technique. *IEEE Trans Biomed Eng* 13: 19–28, 1966.
- Kleine BU, Blok JH, Oostenveld R, Praamstra P, and Stegeman DF. Magnetic stimulation-induced modulations of motor unit firings extracted from multi-channel surface EMG. *Muscle Nerve* 23: 1005–1015, 2000.
- Kukulka CG and Clamann HP. Comparison of the recruitment and discharge properties of motor units in human brachial biceps and adductor pollicis during isometric contractions. *Brain Res* 219: 45–55, 1981.
- Lawrence JH and De Luca CJ. The myoelectric signal versus force relationship in different human muscles. *J Appl Physiol* 54: 1653–1659, 1983.
- LeFever RS and De Luca CJ. Decomposition of superimposed action potential trains. *Proc 8th Annu Meeting Soc Neurosci*, 299, November, 1978.
- LeFever RS and De Luca CJ. A procedure for decomposing the myoelectric signal into its constituent action potentials. Part I. Technique, theory and implementation. *IEEE Trans Biomed Eng* 29: 149–157, 1982.
- Lesser V, Nawab SH, and Klassner F. IPUS: an architecture for the integrated processing and understanding of signals. *Artif Intell* 77: 129–171, 1995.

- Loudon GH, Jones NB, and Sehmi AS.** New signal processing techniques for the decomposition of EMG signals. *Med Biol Eng Comput* 30: 591–599, 1992.
- Mambrito B and De Luca CJ.** A technique for the detection, decomposition and analysis of the EMG signal. *Electroencephalogr Clin Neurophysiol* 58: 175–188, 1984.
- Masakado Y, Akaboshi K, Nagata M, Kimura A, and Chino N.** Motor unit firing behavior in slow and fast contractions of the first dorsal interosseous muscle of healthy men. *Electroencephalogr Clin Neurophysiol* 97: 290–295, 1995.
- Masuda T and De Luca CJ.** Recruitment threshold and muscle fiber conduction velocity of single motor units. *J Electromyogr Kinesiol* 1: 116–123, 1991.
- Masuda T, Miyano H, and Sadoyama T.** A surface sensor array for detecting action potential trains of single motor units. *Electroencephalogr Clin Neurophysiol* 60: 453–443, 1985.
- McGill KC, Cummins KL, and Dorfman LJ.** Automatic decomposition of the clinical electromyogram. *IEEE Trans Biomed Eng* 32: 470–477, 1985.
- McGill KC, Lateva ZC, and Marateb HR.** EMGLAB: an interactive EMG decomposition program. *J Neurosci Methods* 149: 121–133, 2005.
- Moritz CT, Barry BK, Pascoe MA, and Enoka RM.** Discharge rate variability influences the variation in force fluctuations across the working range of a hand muscle. *J Neurophysiol* 93: 2449–2459, 2005.
- Nawab SH and Lesser V.** Integrated processing and understanding of signals. In: *Symbolic and Knowledge-Based Signal Processing*, edited by Oppenheim A and Nawab SH. Upper Saddle River, NJ: Prentice Hall, 1992, p. 251–285.
- Nawab SH, Wotiz R, and De Luca CJ.** Improved resolution of pulse superpositions in a knowledge-based system for EMG decomposition. *Proc 26th Int Conf IEEE Eng Med Biol Soc*, San Francisco, CA, September 2004a, p. 69–71.
- Nawab SH, Wotiz R, and De Luca CJ.** Resolving EMG pulse superpositions via utility maximization. *Proc 8th World Multiconf Systemics, Cybernetics, Informatics*, Orlando, FL, July 2004b, vol. XII, p. 233–236.
- Nawab SH, Wotiz RP, Hochstein LM, and De Luca CJ.** Improved decomposition of intramuscular EMG signals, SCI-2002. *Proc 6th World Multiconf Systemics, Cybernetics, Informatics*, Orlando, FL, July 2002a, vol. XIII, p. 274–279.
- Nawab SH, Wotiz RP, Hochstein LM, and De Luca CJ.** Next-generation decomposition of multi-channel EMG signals. *Proc 2nd Joint Meeting IEEE Eng Med Biol Soc and Biomed Eng Soc*, Houston, TX, October 2002b, p. 36–37.
- Östlund N, Yu J, Roeleveld K, and Karlsson JS.** Adaptive spatial filtering of multichannel surface electromyogram signals. *Med Biol Eng Comput* 42: 825–831, 2004.
- Person RS and Kudina LP.** Discharge frequency and discharge pattern of human motor units during voluntary contraction of muscle. *Electroencephalogr Clin Neurophysiol* 32: 471–483, 1972.
- Roark RM, Schaefer SD, Li JCL, Adam A, and De Luca CJ.** Multiple motor unit recordings of laryngeal muscles. *Laryngoscope* 112: 2196–2203, 2002.
- Rose J and McGill KC.** Muscle activation and motor unit-firing characteristics in cerebral palsy. *Gait Posture* 13: 285–286, 2001.
- Simon W.** The real-time sorting of neuro-electric action potentials in multiple unit studies. *Electroencephalogr Clin Neurophysiol* 18: 192–195, 1965.
- Sogaard K.** Motor unit recruitment pattern during low-level static and dynamic contractions. *Muscle Nerve* 18: 292–300, 1995.
- Stashuk D and de Bruin H.** Automatic decomposition of selective needle-detected myoelectric signals. *IEEE Trans Biomed Eng* 35: 1–10, 1988.
- Tanji J and Kato M.** Firing rate of individual motor units in voluntary contraction of abductor digiti minimi muscle in man. *Exp Neurol* 40: 771–783, 1973.
- Taylor AM and Enoka RM.** Quantification of the factors that influence discharge correlation in model motor neurons. *J Neurophysiol* 91: 796–814, 2004.
- Türker KS, Miles TS, Smith N, and Nordstrom MA.** On-line discrimination of unit potentials on the basis of their waveforms: a new approach implemented on a personal computer. In: *EMG of Jaw Reflexes in Man*, edited by van Steenberghe D and De Laat A. Leuven, Belgium: Leuven Univ. Press, 1989, p. 445–451.
- Von Neumann J and Morgenstern O.** *Theory of Games and Economic Behavior*. Princeton, NJ: Princeton Univ. Press, 1944.
- Westad C and Westgaard RH.** The influence of contraction amplitude and firing history on spike-triggered averaged trapezius motor unit potentials. *J Physiol* 562: 965–975, 2005.
- Windhorst U.** On the role of recurrent inhibitory feedback in motor control. *Prog Neurobiol* 49: 517–587, 1996.
- Winograd JM and Nawab SH.** A C++ software environment for the development of embedded signal processing systems. *ICASSP-95*, Detroit, MI, 1995, p. 2715–2719.
- Zennaro D, Wellig P, Moschytz GS, Läubli T, and Krueger H.** A decomposition software package for the decomposition of long-term multi-channel electromyographic signals. *Proc 23rd Annu Int Conf IEEE Eng Med Biol Soc*, 2001, p. 1070–1073.